RESEARCH ARTICLE

A sensitivity study on the starting simulations of turbojet engines

E. Güllü[1] , G. Aran[1], M. Erk[2] and Ö.U. Baran[2]

[1]Chief Engineering Department, TUSAŞ Engine Industries, Inc., Ankara, Turkey
[2]Mechanical Engineering Department, Middle East Technical University, Ankara, Turkey
Corresponding author: E. Güllü; Email: gulluemrh@gmail.com

Abstract

Gas turbine engine starting models require a lot of calibration to represent reality with acceptable accuracy due to the lack of high-quality component rig data in the sub-idle region. A detailed sensitivity study is presented in this paper to guide such calibration efforts. A thermodynamic component-matching type transient model of a single-spool turbojet engine with shaft and heat-soakage dynamics is employed for this purpose. Turbomachinery component maps are extended to sub-idle using an in-house map smoothing tool and the strategies presented by Kurzke recently. These extension strategies make use of the correlations hidden in the already available regions of the maps and ensure physical consistency. However, they contain some uncertainty, even when an experimentally obtained zero-speed line is available. Combustor sub-idle efficiency, stability limits, and delay are taken from the literature. Due to the chaotic nature of a combustor in the sub-idle region, a precise prediction of the combustor efficiency seems impossible. Effects of uncertainties related to sub-idle turbomachinery map extensions, burner efficiency, and heat soakage are investigated in this paper. Two popular fuel control strategies are employed and compared to see how controls deal with these uncertainties. It is concluded that turbomachinery torque characteristics and turbine capacities are the most important parameters when calibrating a starting model with a control based on rotational acceleration while burner efficiency and heat soakage are added on top of these with a control based on fuel flow rate.

Nomenclature

CFD	computational fluid dynamics
RANS	Reynolds-Averaged Navier Stokes
ECMF	exit corrected mass flow rate
EGV	exit guide vane
PR	pressure ratio
NGV	nozzle guide vane

Symbols

k_1	quadratic constant of zero-speed PR-flowrate curve
W_c	corrected mass flow rate
N	rotational speed
ψ	head coefficient
ϕ	flow coefficient
η	burner efficiency
Ω	burner loading
B	combustor part-load constant for loading

C	combustor part-load constant for corrected flow rate
$\dot{N}$	rotational acceleration
δ_2	compressor inlet corrected total pressure
w_f	fuel flow rate
P_3	compressor exit total pressure
θ_2	compressor inlet corrected total temperature
T_3	compressor exit total temperature
T_5	turbine exit total temperature
τ	heat soakage time constant
C_D	nozzle discharge coefficient

1.0 Introduction

Sub-idle engine operation refers to the operation between fully static and stabilised-idle conditions. An electric starter is usually employed to crank the engine and send enough air to ignite the combustor. Starter support continues until the engine can self-sustain and reach the idle speed on its own. Fundamental processes happening in a gas turbine engine during the sub-idle operation are not very different from the above-idle operation. However, uncertainties related to the component performances are higher in the sub-idle regime due to the lack of high-quality component rig data. Most flow solvers and performance correlations are also tuned for above-idle operation. Due to these challenges, the sub-idle performance estimation of gas turbine engines is still an understudied topic.

Early studies for turbomachinery sub-idle map extension, such as Refs [1] and [2], used simple extrapolation techniques based on incompressible-flow similarity laws. Riegler et al. [3] also used a similar technique; however, they checked their results using some physical judgment. A review of different sub-idle compressor map extrapolation techniques is provided by Jones et al. [4].

Recent studies prefer to compute or estimate zero-speed curves and employ interpolation rather than extrapolation. Howard [5], Zachos [6], Zachos et al. [7], and Grech [8] interpolated sub-idle compressor maps using computed zero-speed curves, which are generated using loss coefficients from CFD analysis. They also investigated sub-idle combustor behaviour, which is rare in the literature. They concluded that the commonly used reaction-controlled combustor efficiency formula is insufficient for sub-idle, and fuel evaporation effects should be accounted for.

Ferrer et al. [9] designed an axial compressor rig to obtain zero-speed and windmilling characteristics. This data was used to generate a sub-idle compressor map by interpolation, which was then compared with existing extrapolation techniques. The computation of zero-speed and zero-torque curves for an axial compressor was investigated by Righi et al. [10] using two different low-order models, which were validated with 3D RANS CFD and experimental results. A sub-idle map interpolation strategy using these computed zero-speed and zero-torque curves was presented by Ferrer et al. [11]. This study employed a physically sound coordinate, the exit corrected mass flow rate (ECMF), as one of the interpolation coordinates along with the corrected speed. Previous studies usually employed an auxiliary coordinate, called beta lines, instead of ECMF lines.

The effect of interstage bleed on compressor characteristics for sub-idle speeds is investigated experimentally, numerically and analytically by Tio et al. [12]. A low-order meanline model is shown to correctly capture this effect. This meanline model is combined with an interpolation strategy, as explained by Ferrer et al. [9], to form sub-idle maps with different interstage bleed settings. Both normal and reverse bleed flow scenarios are considered. Reverse bleed flow can happen since sub-atmospheric pressures can be seen in the engine core during windmilling.

Kurzke and Marie [13] developed a compressor sub-idle map interpolation strategy that requires no detailed geometry information. Zero-speed curves are guessed and later checked by various correlations embedded in the map to be extended. The incompressible-flow theory was used with some compressibility corrections based on exit guide vane (EGV) Mach numbers. The linear relationship between specific corrected torque and corrected mass flow rate, with a slope independent of speed, was used

to extend torque maps. There are very few studies about sub-idle turbine map extension and the most detailed study about this topic was conducted by Kurzke [14]. He used the incompressible-flow theory together with some judgment about zero-flow and unity-PR characteristics. Again this procedure requires no detailed geometrical information. Recently, Kurzke [15] published an improvement for his compressor extension strategy for very low speeds. Extending the compressor maps to spool speeds of less than 10% is challenging because the use of work and flow coefficient correlations become too sensitive. This is solved by Kurzke [15] by introducing a second set of beta lines for such low speeds. These lines represent constant flow coefficient points. The region between 0-speed and torque-free windmilling lines is not covered by such a beta-line grid, which can be a problem especially for low pressure compressors.

Whole engine modeling studies to predict sub-idle performance started with simple operating line extrapolation models, also called torque models. These models are based on extrapolated steady-state component operating lines, hence requiring no component maps. Transient excursions are modeled empirically. Examples of such models are given by Agrawal and Yunis [16], Walsh and Fletcher [17], and Morini et al. [18]. These models can be used as a preliminary tool to estimate starter power requirements; however, they are not enough to accurately estimate station parameters.

One of the earliest studies that used a detailed thermodynamic sub-idle model with extended component maps was conducted by Chappell and McLaughlin [19]. This model was based on thermodynamic matching and the compressor map was extended using a streamline curvature program and a guess for zero-speed curves. Turbine map extension and combustor stability considerations were also included in the study. A similar, but more detailed, study was presented by von et al. [20]. They developed a transient model for a free-turbine turboshaft engine, which can also simulate sub-idle operation. A detailed calibration of heat soakage and tip clearance characteristics was made, which was necessary to obtain an acceptable agreement with test data. They also had to improve their combustor model by including evaporation-controlled efficiency, which becomes dominant during sub-idle operation.

A more recent study was presented by Bretschneider and Reed [21]. They developed a sub-idle thermodynamic turbofan model, tackling turbofan-specific challenges of modeling fully static conditions, static friction and reverse flows. They showed that expected trends can be captured; however, they did not present any detailed test comparison. Jia and Chen [22] developed and validated a sub-idle model for an Allison 250 turboshaft engine using ideas presented by Zachos [6]. An interesting study conducted by Ferrand et al. [23] employed a detailed sub-idle model for a new twin-engine helicopter flight mode. In this mode, one engine is kept at a low sub-idle speed with an electric motor and restarted when needed. Besides flow path components, they also employed detailed models for secondary air flows, subsystems and controls. Simulations were compared with test data, correctly predicting trends.

Kurzke [15, 24] presented a starting and windmilling model for a mixed-flow turbofan engine using his previously developed component extension strategies. These strategies were tested in this study, showing that they indeed produce physically sound maps. It was claimed that precise calculation of combustor efficiency is not required for sub-idle models. In other words, sub-idle operating lines are relatively insensitive to combustor efficiency. However, this might be because the author employed a fuel control strategy based on rotational acceleration, but not on fuel flow rate. Numerical tricks to improve model convergence were presented in detail. Although no test data comparison was given, it was stated that deviations from test data are expected due to the uncertainties of parasitic losses, combustor light-up efficiency and extended component maps.

Previous studies confirm that thermodynamic sub-idle models with carefully extended turbomachinery maps can capture the expected trends. However, due to the uncertainties of the extensions, they require some calibration to represent reality with acceptable accuracy. A detailed sensitivity study for a single-spool turbojet engine is presented in this paper, aiming to guide such calibration efforts. First, the methodologies related to turbomachinery map extensions, burner performance, transient engine modeling and fuel control strategies are explained. Then, a steady-state analysis is laid out to ensure the extended maps are physically consistent. This analysis is also used to size an electric starter and to
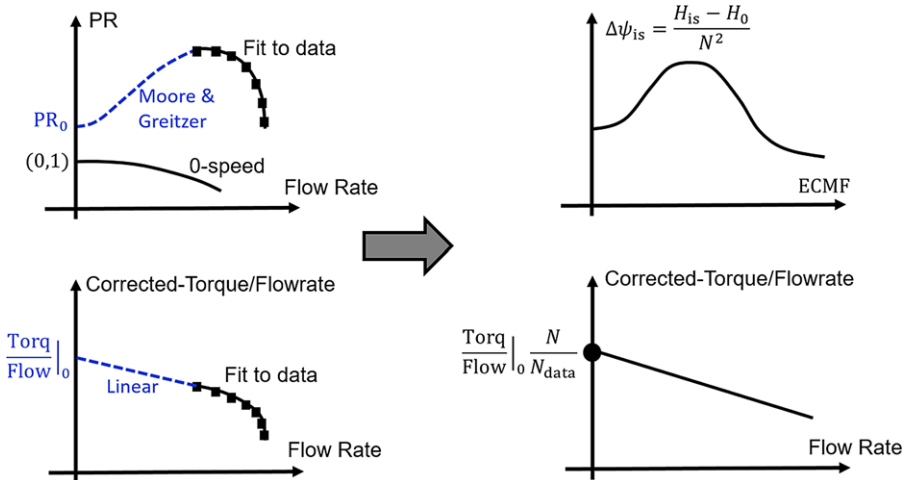
Figure 1. *The initial guess procedure used for a compressor.*

design fuel control schedules. Finally, a transient engine model is used to assess the effects of uncertainties related to the component performances and heat soakage. Two popular fuel control strategies are employed and compared to see how controls deal with these uncertainties.

2.0 Methodology

2.1 Sub-idle turbomachinery maps

Sub-idle turbomachinery maps are obtained from above-idle map data using methodologies explained by Kurzke and Marie [13] and Kurzke [14]. These methodologies make use of the incompressible-flow similarity laws together with some physical judgment for compressibility effects. Specific torque (torque/flowrate) maps are employed instead of efficiency maps since their behaviour is more predictable in the sub-idle regime. The zero-speed curves are guessed and later checked by the physical consistency of the resulting map. Details of these methodologies are well explained by Kurzke and will not be repeated here.

We have developed an initial estimation procedure that can generate sub-idle maps automatically from a single high-speed data and a guessed or computed zero-speed PR-flowrate curve. Maps obtained with this procedure require minimal adjustment for the incompressible part of PR-flowrate curves and the compressible part of torque/flowrate-flowrate curves. This adjustment is done via an in-house tool that employs Bezier curves to enable manual adjustments. Referring to Fig. 1, the initial estimation procedure for a compressor works as follows. First, the available speed data is extended to zero-flow using Moore and Greitzer's cubic characteristics [25] and linearity of torque/flowrate data. Then, relative isentropic head coefficients ($\Delta\psi_{is}$) and normalised torque/flowrate data are plotted against ECMF ($W_c\sqrt{T_3}/P_3$) and flow rate respectively. Finally, these curves can be used to obtain PR and torque characteristics for any speed. This requires an iterative procedure, which can be summarised as:

1. Form a grid between zero and maximum ECMF.
2. Compute PR from the relative isentropic head coefficient curve for each ECMF.
3. Guess flow rate and compute torque from normalised torque/flowrate curve.
4. Repeat step 3 and iterate flow rate until target ECMF is met for each ECMF.
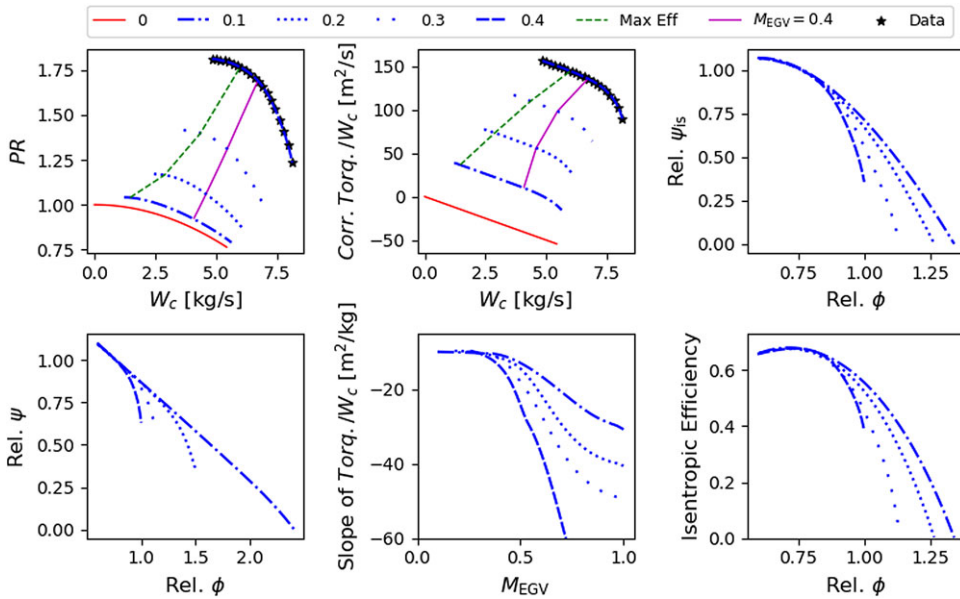5. Repeat steps 2-4 for each sub-idle speed.

**Figure 2.** *A compressor sub-idle map extended using the above-explained methodology.*

A compressor map obtained with this procedure is shown in Fig. 2 with some key figures to check the physical consistency of the resulting map. As can be seen, $\psi - \phi$ and $\psi_{is} - \phi$ curves are unique, and torque/flowrate curves are linear in the incompressible region. Figure 2 also shows the correlation of compressibility effects with EGV Mach number. A similar procedure is used for turbines by replacing ECMF with inlet-corrected mass flow rate.

Although the above-idle data can be used to infer the slope of the zero-speed torque/flowrate curve, it provides little information for the zero-speed PR-flowrate curve for a compressor. Zero-speed PR-flowrate curves are known to follow a quadratic trend ($PR = 1 - k_1 W_c^2$). Several sub-idle maps are formed by changing the quadratic constant, k_1, to see if the resulting map can give us clues about the true value of k_1. It is observed that the linearity of the peak efficiency curve on the torque/flowrate plot is lost for low values of k_1. However, it is not possible to converge into a single value of k_1, and physically consistent maps can be obtained for a wide range of k_1 values. Even when a computationally or experimentally obtained zero-speed PR-flowrate curve is available, the compressible part of PR-flowrate curves cannot be fixed exactly and contain some uncertainty.

The above-mentioned concerns are less of an issue for a turbine since PR-flowrate trends are more obvious from the above-idle data. A turbine is expected to choke from NGV for sub-idle speeds and choking mass flow rate is known from the lowest-available above-idle speed data. As speed decreases, NGV chokes at a lower PR since NGV has a higher PR for the same overall PR. This trend continues until a quadratic zero-speed curve is reached. Zero-flow and unity-PR characteristics are also helpful to extend turbine maps to low-flow and low-PR regions, as explained by Kurzke [14].

2.2 Combustor sub-idle performance

The classical loading-based formula that works for above-idle operation predicts unrealistic light-up efficiencies (combustor efficiency during and just after its ignition). This problem stems from the fact that the evaporation process, rather than the reaction process, is the dominant process during and just after light-up [5]. A formula is given by Lefebvre [26] for the evaporation rate-controlled efficiency. However, this formula requires some inputs that are hard to estimate, such as droplet diameter and
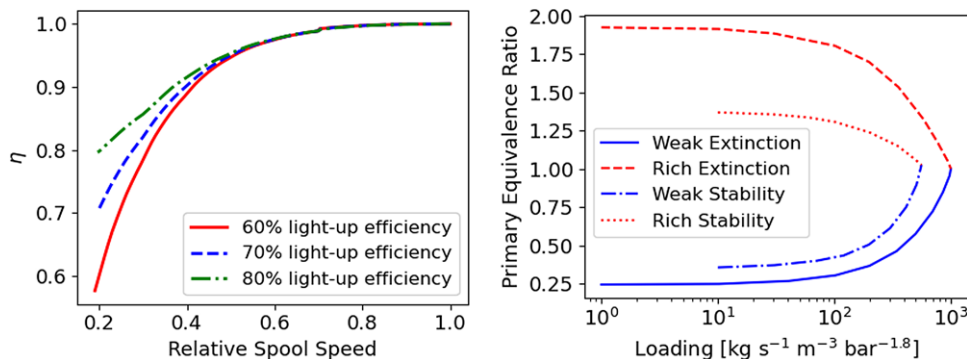
Figure 3. *Burner efficiency (left) and burner stability (right) curves used in this study.*

evaporation constant. If these inputs are assumed constant, the rest resemble the corrected mass flow rate. Therefore, the following formula is proposed in this study to include evaporation effects in the classical loading-based formula:

$$\eta = 1 - \exp\left(\log\left(1 - \eta_{ds}\right) + B \log\left(\frac{\Omega}{\Omega_{ds}}\right) - C \log\left(\frac{W_c}{W_{c,ds}}\right) \right) \tag{1}$$

Here, η, Ω, and W_c are the combustor efficiency, the combustor loading, and the corrected mass flow rate, respectively. Subscript ds represents the design conditions. B and C are the part-load constants that define off-design efficiency drops. Adding the last term in Equation (1) provided a way to model efficiency drop due to evaporation effects. The usage of flow rate as an inefficiency factor is also mentioned by Grech [8].

Burner efficiencies during and just after light-up are hard-to-predict and rarely mentioned in the literature. Walsh and Fletcher [17] reported that they are expected to be in the range of 60-80%. Based on this information, Equation (1) is adjusted to give the curves shown in Fig. 3. Besides efficiency, combustor stability is also quite crucial for sub-idle performance assessments, and stability curves given by Walsh and Fletcher [17] are used for this purpose, as shown in Fig. 3.

2.3 Transient component matching

A thermodynamic component-matching type transient performance model with shaft and heat-soakage dynamics is employed for the simulations. Newton-Raphson iterations are utilised for the flow matching and dynamic equations are solved with the simple forward Euler method, as shown in Fig. 4. Volume dynamics are ignored since they die out quickly for a relatively slow sub-idle transient manoeuver. Tip clearance changes can have significant effects on component performances; however, it is hard to quantify these effects for such off-design conditions and they are ignored in the current study. This assumption will show itself as an extra uncertainty in turbomachinery performance curves.

2.4 Control of starting

A simple min-max type fuel control strategy is used as shown in Fig. 5. Here the closed-loop corrected rotational acceleration ($\dot{N}/\delta_2$) control can be replaced by an open-loop corrected fuel flow rate (w_f/P_3) control. $\dot{N}/\delta_2$ and w_f/P_3 are the two most common transient control strategies and they are both scheduled against corrected speed ($N/\sqrt{\theta_2}$). Controller gains are found by trial and error. The set point controller (N controller) loop targets the idle speed, which is 70% in this study, and aims for the engine to reach stabilised idle condition while the transient controller ($\dot{N}/\delta_2$ or w_f/P_3 controller) loop protects the engine from surge, flameout and high temperatures. The choice of using $\dot{N}/\delta_2$ or w_f/P_3 for
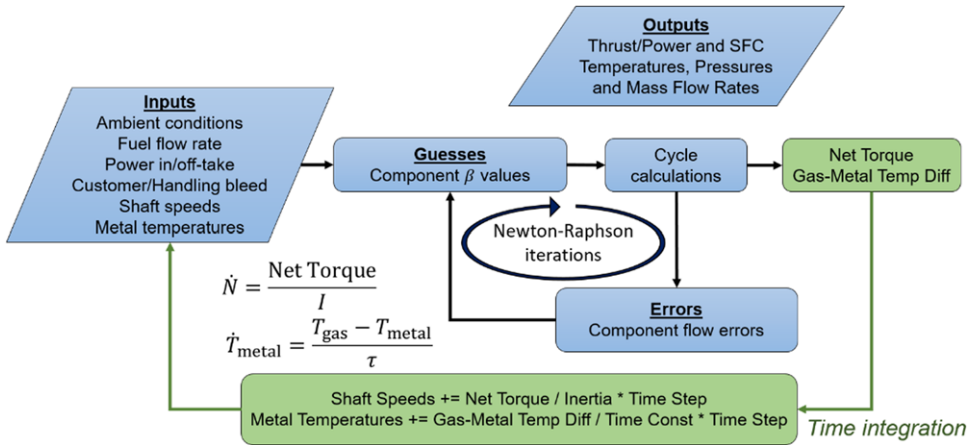
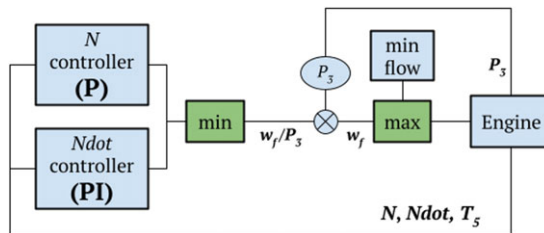**Figure 4.** *Transient component matching algorithm.*

Figure 5. *Min-max type fuel control strategy employed in this study.*

the fuel control and its effect on the expected uncertainties will be discussed in the following sections. It is expected that $\dot{N}/\delta_2$ control will give a consistent starting time while w_f/P_3 control will provide better protection from surge and stall.

3.0 Results and Discussions

Results and discussions that will be presented in this section are obtained for a single-spool turbojet configuration as shown in Fig. 6. Basic cycle parameters and above-idle component maps are obtained from GasTurb's [27] standard turbojet model. This model has a corrected compressor inlet mass flow rate of 32kg/s, a pressure ratio of 12, and a burner exit temperature of 1,450K to produce roughly 26kN thrust at sea-level static conditions. Burner volume, which is needed by burner stability assessments, is taken as 0.1m^3 in order to have a reasonable design point burner loading. Shaft inertia is scaled from a known engine and taken as 5kgm^2. Twenty per cent handling bleed is employed to have enough surge margin for sub-idle accelerations.

Extended compressor maps for 3 different k_1 values, which can all give a physically consistent map, are shown in Fig. 7. As can be seen, the compressible part of PR-flowrate curves can vary quite considerably for different values of k_1. The extended turbine map is given in Fig. 8.

3.1 Steady-state analysis

A steady-state analysis within the sub-idle region can be used to assess if the extended maps are physically consistent. It can also be used to estimate the required starter power and fuel schedule. Steady-state
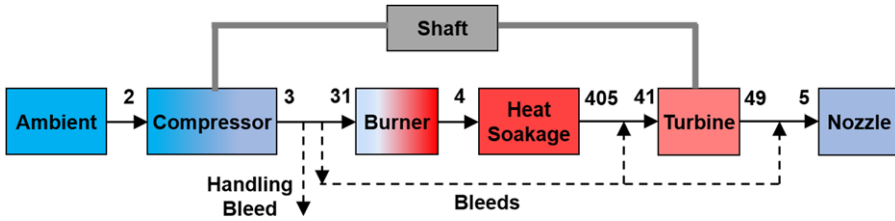
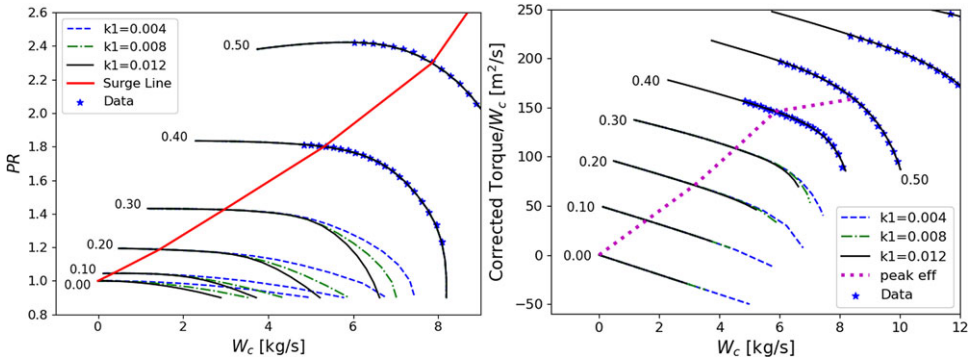**Figure 6.** *Single-spool turbojet configuration.*

Figure 7. *Extended compressor map with different k_1 values.*
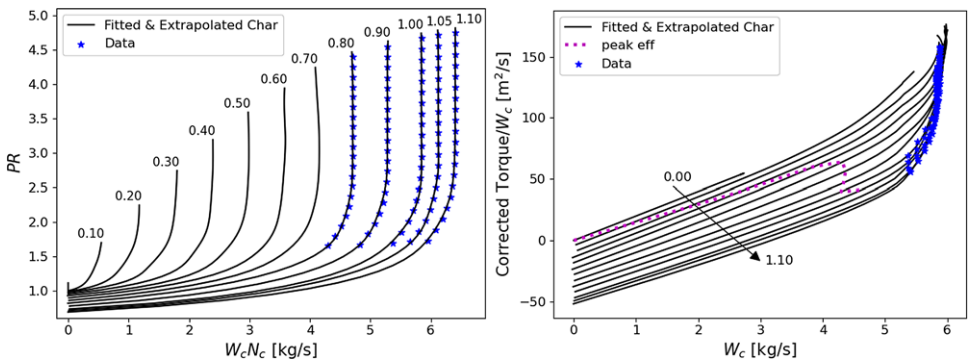

Figure 8. *Extended turbine map.*

compressor operating, cranking, and windmilling lines are shown in Fig. 9. Steady-state results are obtained by replacing dynamic equations in Fig. 4 with an iteration for the shaft power balance. This balance is achieved by adjusting the fuel flow rate for the operating line, starter power for the cranking line and Mach number for the windmilling line. Numerical convergence can be achieved down to 2–3% compressor speed for the operating and windmilling line and 0.1% compressor speed for the cranking line. This gives confidence that the extended maps will give us no numerical problems.

Fuel schedules are formed by simulating transient conditions with a steady-state power offtake. An iteration is formed that adjusts power offtake to reach a defined operational limit. The considered limits are surge margin limit of 10%, turbine exit temperature (T_5) limit of 1,150K, and combustor extinction limits defined in Fig. 3. $\dot{N}/\delta_2$ and w_f/P_3 values corresponding to these limits and the initial schedules formed can be seen in Fig. 10. It is important to note that fuel schedules are obtained using a nominal value of 70% for light-off burner efficiency.
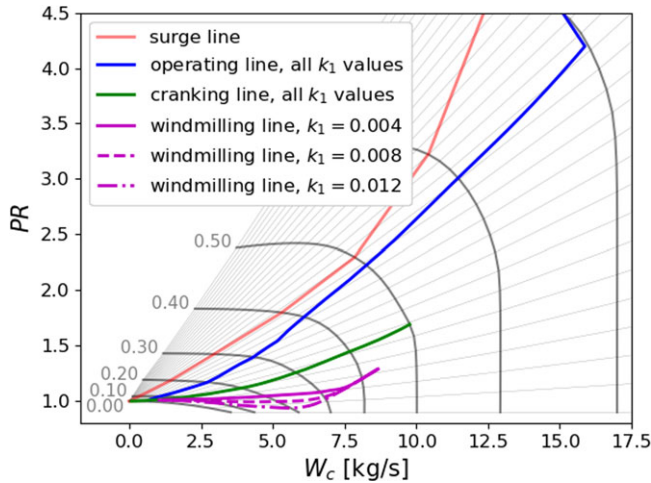
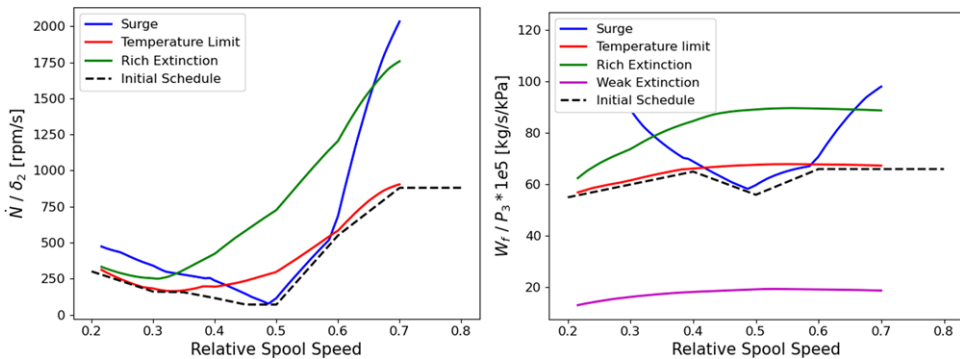**Figure 9.** *Steady-state operating, cranking and windmilling lines.*

Figure 10. *Limits used to define an initial fuel schedule for $\dot{N}/\delta_2$ and w_f/P_3 control strategies.*

3.2 Transient analysis

First, a transient simulation is conducted starting from the static conditions to see if the schedules perform reasonably well. Obtained results using the $\dot{N}/\delta_2$ schedule are given in Fig. 11. As can be seen, all the defined limits are respected and the same is also true for the w_f/P_3 schedule. Next, a sensitivity study is performed using both schedules to see how the uncertainties related to different modeling parameters affect the end result of a starting simulation and how controls deal with these uncertainties. This will be detailed for each modeling parameter in the following.

3.2.1 Effect of compressor k_1

The compressor k_1 value was used to construct a zero-speed line, and it was shown that it can affect the interpolation of sub-idle PR-flowrate characteristics significantly within the compressible region. Luckily, most of the starting happens in the incompressible region. Only some portion of the cranking happens in the compressible region, which has a very slight effect (around 1%) on the time-to-reach-idle. Since the cranking line is not affected by compressor characteristics, it is unique for all k_1 values. Therefore; the selection of the compressor k_1 value is not that significant for starting simulations of single-spool engines. However, its effect can be significant if there is a windmilling compressor during starting, which is the case for engines with multi-spool compressor configurations. Steady operating,
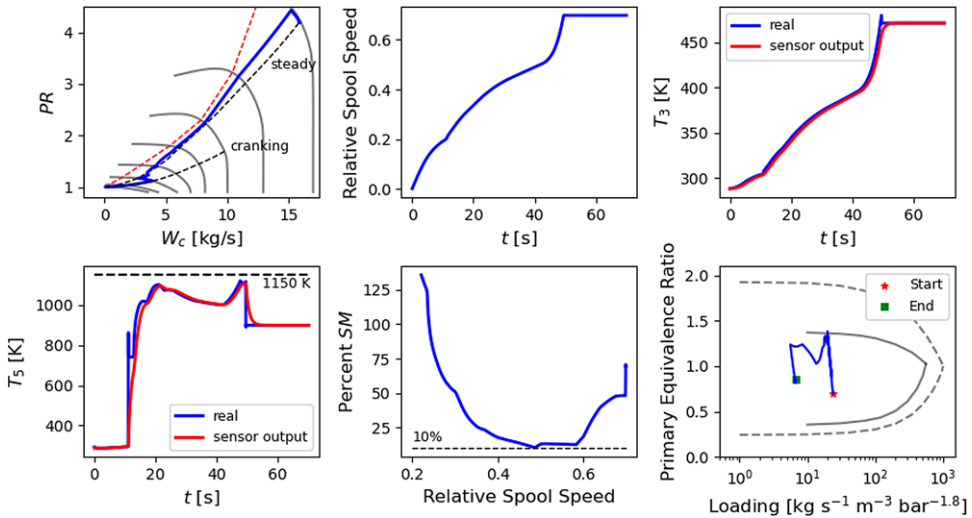
Figure 11. *Transient analysis results using $\dot{N}/\delta_2$ control.*

cranking and windmilling lines for different k_1 values can be seen in Fig. 9, which explains why we expect a significant k_1 effect for a windmilling compressor, but not for a cranking compressor.

3.2.2 Effect of flow capacities

Turbine flow-capacity change has an important effect on the operating line and surge margin for both control strategies. Its effect on temperature levels is relatively slight, while the starting time (time-to-reach-idle) is affected significantly for w_f/P_3 control. Figure 12 shows the results for different turbine capacities using $\dot{N}/\delta_2$ control. Although not clear from Fig. 12, turbine flow-capacity change can affect the cranking operating line, and it is the main calibration parameter for cranking line adjustment.

Compressor-flow capacity change does not affect the operating line and its effect on temperatures is very slight. The starting time is again affected significantly for w_f/P_3 control. Figure 13 shows the results for different compressor capacities using w_f/P_3 control.

Uncertainty of nozzle discharge coefficient (C_D) for sub-idle operation gives very similar results to turbine capacity; however, they are much less dramatic. It is important to mention that T_5 levels are increased as turbine capacity is increased while the opposite is true for nozzle capacity.

3.2.3 Effect of burner efficiency and heat soakage

Sub-idle burner efficiencies and heat soakage does not affect station parameters and operating lines when $\dot{N}/\delta_2$ control is used since it can adjust the fuel flow rate to compensate for these changes. However, burner efficiencies and heat soakage can affect the T_5 profile and the starting time for w_f/P_3 control. This can be seen in Fig. 14 for burner efficiency. The operating line is almost unique for both control strategies.

3.2.4 Effect of torque characteristics

A change in both compressor and turbine torque characteristics gives very similar results. The only way to distinguish the source of torque change is to check the T_3 profile, which is affected more by compressor torque characteristics. $\dot{N}/\delta_2$ control gives a constant starting time; however, the operating line and temperatures are affected significantly. w_f/P_3 control gives a constant operating line; however, the starting
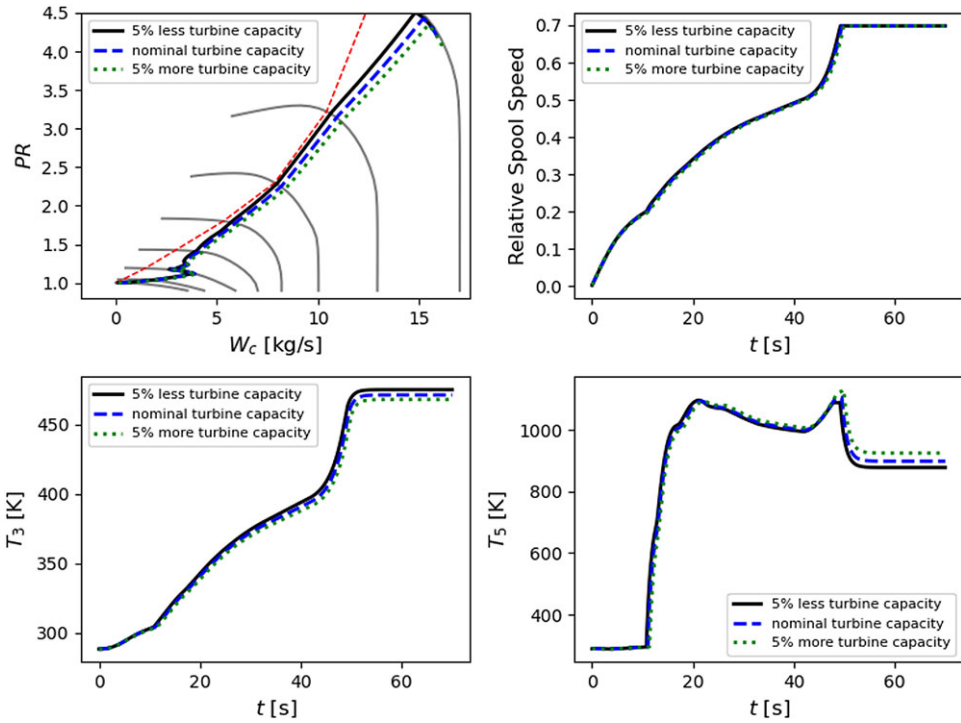
Figure 12. *Operating line, speed profile and temperature profiles for different turbine capacities using $\dot{N}/\delta_2$ control.*
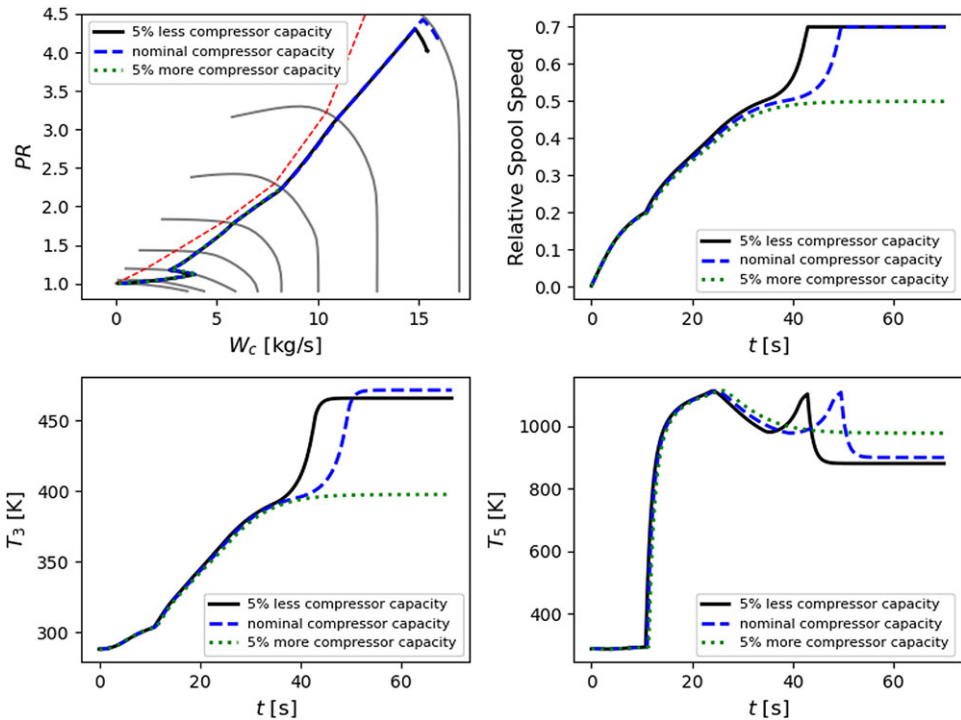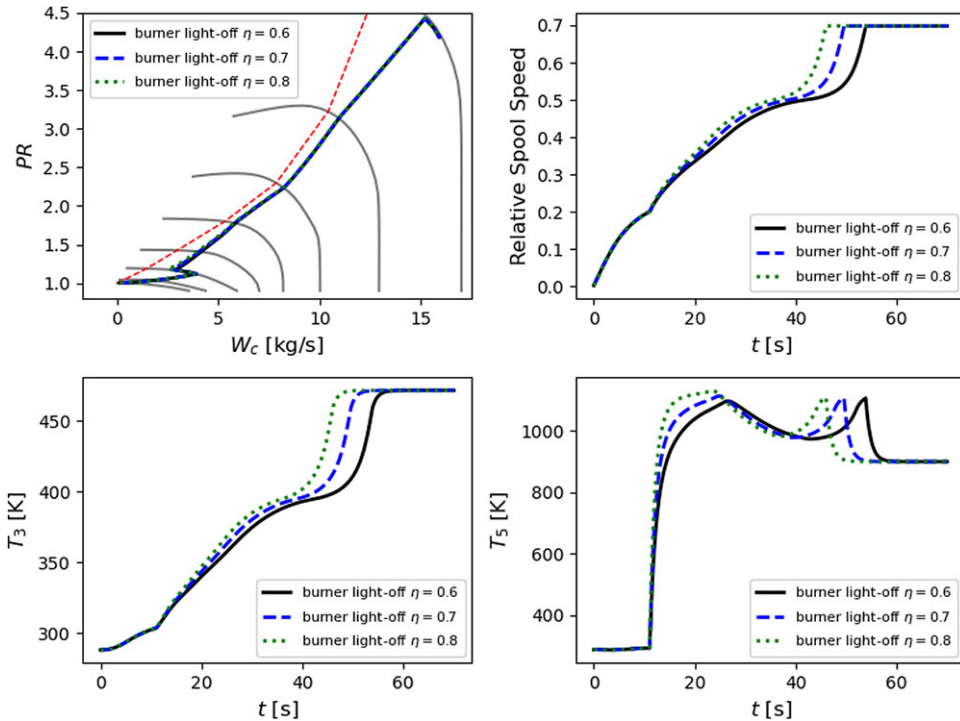

Figure 13. *Operating line, speed profile and temperature profiles for different compressor capacities using w_f/P_3 control. Five per cent more capacity case hangs.*

Figure 14. *Operating line, speed profile and temperature profiles for different burner efficiencies using* w_f/P_3 *control.*

time and temperatures are affected significantly this time. Figure 15 shows how compressor torque characteristics affect the results for $\dot{N}/\delta_2$ control while Figure 16 shows how turbine torque characteristics affect the results for w_f/P_3 control.

Sub-idle torque losses are not modeled in this study since they will not have a considerable effect on the obtained results. When they are modeled properly, they can be significant during cranking and windmilling, especially for certain atmospheric conditions. However, sub-idle torque losses become very small compared to turbine and compressor torques after light-up.

3.3 Discussions

Tables 1 and 2 summarise the sensitivity study performed above. The main takeaways are as follows:

- The compressor k_1 value, which controls the compressible part of sub-idle PR-flowrate characteristics, cannot be fixed exactly using above-idle data. Luckily, it has little effect on single-spool turbojet engine starting simulations. It is expected to have more effect when there is a windmilling compressor.
- Turbine capacity uncertainties can have significant effects on the operating line and the starting time while compressor and nozzle capacity has relatively little effect. Temperature levels are affected slightly by capacity changes.
- Burner efficiency and heat soakage are effective on the starting time and the T_5 profile when w_f/P_3 control is used. When $\dot{N}/\delta_2$ control is used, they show no effect. The operating line is almost unique for both control strategies.
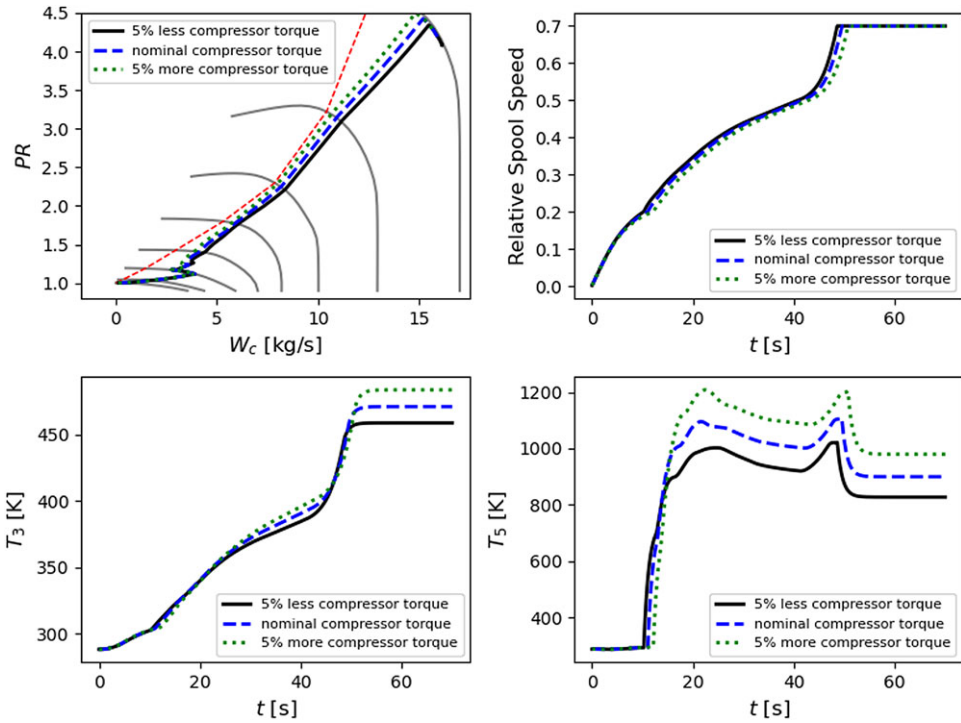
Figure 15. *Operating line, speed profile and temperature profiles for different compressor torque characteristics using $\dot{N}/\delta_2$ control.*
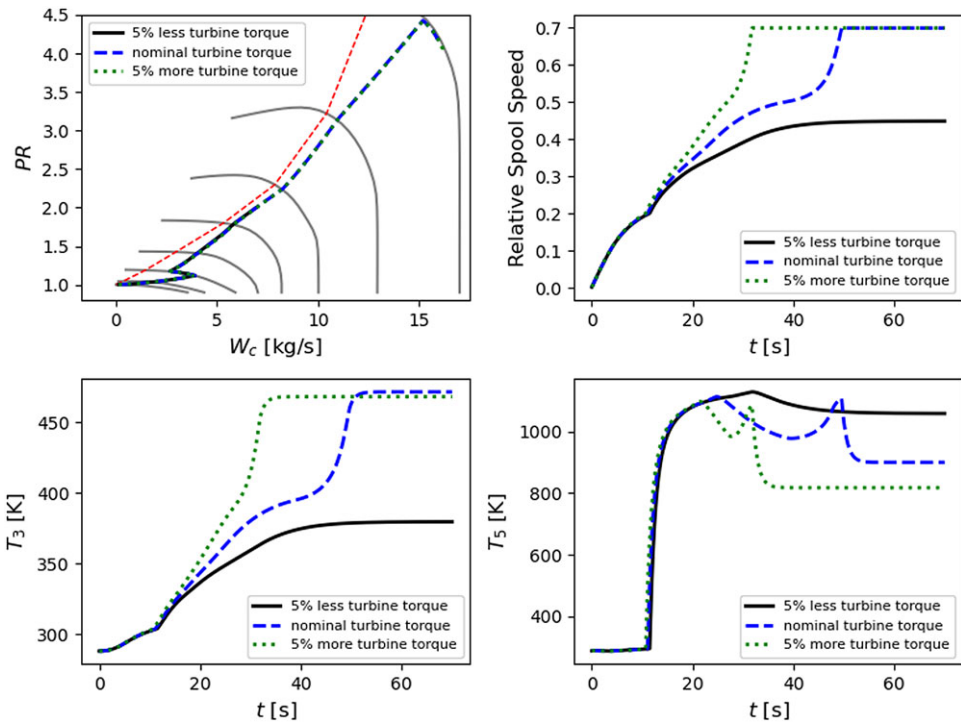

Figure 16. *Operating line, speed profile and temperature profiles for different turbine torque characteristics using w_f/P_3 control. Five per cent less turbine torque case hangs.*

Table 1. *Summary of the sensitivity study using $\dot{N}/\delta_2$ control*

Modeling parameter	Compressor operating line	T5 profile	Time-to-reach-idle
Compressor k_1	No effect	No effect	No effect
Turbine capacity	Significant effect	Effect	No effect
Compressor capacity	No effect	Slight effect	No effect
Burner efficiency	No effect	No effect	No effect
Compressor torque	Significant effect	Significant effect	Slight effect
Turbine torque	Significant effect	Significant effect	Slight effect
Heat soakage τ	No effect	No effect	No effect
Nozzle C_D	Effect	Effect	No effect

Table 2. *Summary of the sensitivity study using w_f/P_3 control*

Modeling parameter	Compressor operating line	T5 profile	Time-to-reach-idle
Compressor k_1	No effect	No effect	No effect
Turbine capacity	Significant effect	Effect	Significant effect
Compressor capacity	No effect	Slight effect	Significant effect
Burner efficiency	No effect	Effect	Effect
Compressor torque	No effect	Significant effect	Significant effect
Turbine torque	No effect	Significant effect	Significant effect
Heat soakage τ	No effect	Effect	Effect
Nozzle C_D	No effect	Effect	Effect

- Uncertainty of both compressor and turbine torques exhibits very significant effects on the operating line, the starting time and the T_5 profile. A change in both compressor and turbine torque characteristics gives similar results, the main difference being the T_3 profile.
- The effects of uncertainties strongly depend on the utilised fuel control strategy. $\dot{N}/\delta_2$ control guarantees a speed profile and a starting time while w_f/P_3 control guarantees an operating line, except for turbine capacity changes.
- Turbomachinery torque characteristics and turbine capacity are the most important parameters for $\dot{N}/\delta_2$ control while burner efficiency and heat soakage are also added on top of these for w_f/P_3 control. Therefore, it is easier to calibrate a starting model for an engine with $\dot{N}/\delta_2$ control.
- Since a compressor acts to compensate pressure losses through the rest of the engine during cranking, its cranking line is only affected by PR-flowrate characteristics of turbines and ducts.

4.0 Conclusions

Original equipment manufacturers (OEMs) of the gas turbine industry have heavily relied on engine testing to investigate the operation in the sub-idle region. However, the definition of safe and optimal starting procedures can be made more practically with the help of a sub-idle model. A detailed sensitivity study, together with novel extension strategies for compressor and burner characteristics, is presented in this paper to guide the calibration efforts of such models. Effects of uncertainties related to sub-idle turbomachinery map extensions, burner efficiencies and heat soakage are investigated, together with a comparison of two popular fuel control strategies. Depending on the control strategy used, recommendations are made that can help to identify the sources of modeling errors.

It is concluded that turbomachinery torque characteristics and turbine capacities are the most important parameters when calibrating a starting model with a control based on rotational acceleration. Since temperature levels are mainly affected by torque characteristics, it is advised to first calibrate

for the temperature profiles using them. Later, operating lines can be calibrated using turbine capacities. Burner efficiency and heat soakage are effective on temperature profiles if a control based on fuel flow rate is used. This makes the calibration process harder, but still manageable.

As a future work, the obtained results will be used to calibrate a starting model for a real turboshaft engine with test data. It is also planned to make a similar sensitivity study for a turbofan engine, with a windmilling fan during starting. This windmilling can make the zero-speed line choice a more important matter.

References

[1] Sexton, W.R. A Method to Control Turbofan Engine Starting by Varying Compressor Surge Valve Bleed, Blacksburg Virginia: M.Sc., Virginia Polytechnic Institute and State University, 2001.

[2] Gaudet, S.R. and Gauthier, J.E. A simple sub-idle component map extrapolation method, ASME Turbo Expo 2007, GT2007-27193, Montreal, 2007.

[3] Riegler, C., Bauer, M. and Kurzke, J. Some aspects of modeling compressor behavior in gas turbine performance calculations, *J. Turbomach.*, 2001, **123**, (2), pp 372–378.

[4] Jones, G., Pilidis, P. and Curnock, B. Extrapolation of compressor characteristics to the low-speed region for sub-idle performance modelling, ASME Turbo Expo 2002, GT2002-30649, Amsterdam, The Netherlands, 2002.

[5] Howard, J. Sub-idle Modelling of Gas Turbines: Altitude Relight and Windmilling, PhD Thesis, Cranfield University, UK, 2013.

[6] Zachos, P.K. Gas Turbine Sub-idle Performance Modelling, PhD Thesis, Cranfield University, UK, 2010.

[7] Zachos, P.K., Aslanidou, I., Pachidis, V. and Singh, R. A sub-idle compressor characteristic generation method with enhanced physical background, *J. Eng. Gas Turbines Power.*, 2011, **133**, (8), p 081702.

[8] Grech, N. Gas Turbine Sub-Idle Performance Modelling; Groundstart, PhD Thesis, Cranfield University, UK, 2013.

[9] Ferrer-Vidal, L., Pachidis, V. and Tunstall, R. An enhanced compressor sub-idle map generation method, Proceedings of GPPS Forum 2018, Zürich, 2018.

[10] Righi, M., Ferrer-Vidal, L. and Pachidis, V. Body-force and mean-line models for the generation of axial compressor sub-idle characteristics, *Aeronaut. J.*, 2020, **124**, (1281), pp 1683–1701.

[11] Ferrer-Vidal, L., Pachidis, V. and Tunstall, R. Generating axial compressor maps to zero speed, *Proc. Inst. Mech. Eng. Part A J. Power Energy*, 2020, **235**, (5), pp 956–973.

[12] Tio, F., Ferrer-Vidal, L., Aguirre, H. and Pachidis, V. Considerations on axial compressor bleed for sub-idle performance models, ASME Turbo Expo GT2020-14413, Online, 2020.

[13] Kurzke, J. and Marie, D. Generating compressor maps to simulate starting and windmilling, ISABE-2019-24299, Canberra, Australia, 2019.

[14] Kurzke, J. (2020). Turbine Map Extension – Theoretical Consideration and Practical Advice. *J. Glob. Power Propuls. Soc.*, **4**, pp 176–189.

[15] Kurzke, J. An enhanced compressor map extension method suited for spool speeds down to 1%, Glob. Power Propuls. Soc. TC-2023-0236, Hong Kong, 2023.

[16] Agrawal, R.K. and Yunis, M. A generalized mathematical model to estimate gas turbine, *J. Eng. Power.*, 1982, **104**, (1), pp 194–201.

[17] Walsh, P. and Fletcher, P. *Gas Turbine Performance*., Blackwell Publishing, 2004, UK.

[18] Morini, M., Cataldi, G., Pinelli, M. and Venturini, M. A model for the simulation of large-size single-shaft gas turbine start-up based on operating data fitting, ASME Turbo Expo 2007, GT2007-27373, Montreal, Canada, 2007.

[19] Chappell, M.A. and McLaughlin, P.W. Approach to modeling continuous turbine engine operation from startup to shutdown, *J. Propuls. Power*, 1993, **9**, (3), pp 466–471.

[20] von Frowein, J., Abdullahi, H., Erhard, W. and Schmidt, K. Design and validation of a real-time model for steady-state and transient performance simulation of a helicopter engine, ISABE2007-1125, Beijing, China, 2007.

[21] Bretschneider, S. and Reed, J. Modeling of start-up from engine-off conditions using, ASME Turbo Expo 2015, GT2015-43528, Montreal, Canada, 2015.

[22] Jia, L. and Chen, Y. Validation of a physically enhanced sub idle compressor map extrapolation method, 16th ISROMAC, USA, 2016.

[23] Ferrand, A., Bellenoue, M., Bertin, Y., Cirligeanu, R., Marconi, P. and Calvairac, F. High fidelity modeling of the acceleration of a turboshaft engine during a restart, ASME Turbo Expo GT2018-76654, Oslo, Norway, 2018.

[24] Kurkze, J. Starting and windmilling simulations using compressor and turbine maps, *J. Glob. Power Propuls. Soc.*, 2023, **7**, pp 58–70.

[25] Moore, F. and Greitzer, E. A theory of post-stall transients in axial compression systems: Part I-development of equations, *J Eng Gas Turbine Power*, 1986, **108**, (1), pp 68–76.

[26] Lefebvre, A. Fuel effects on gas turbine combustion - ignition, stability, and combustion efficiency, *J. Eng. Gas Turbines Power*, 1985, **107**, (1), pp 24–37.

[27] Kurzke, J. Advanced user-friendly gas turbine performance calculations on a personal computer, ASME, International Gas Turbine and Aeroengine Congress and Exposition, Houston, Texas, 1995.